Geomechanics and Engineering, *Vol. 30, No. 2 (2022) 211-218*
https://doi.org/10.12989/gae.2022.30.2.211

A comprehensive laboratory compaction study: Geophysical assessment

Junghee Park[1], Jong-Sub Lee[1], Byeong-Su Jang[2], Dae-Hong Min[2] and Hyung-Koo Yoon[*2]

[1]*School of Civil, Environmental and Architectural Engineering, Korea University 145, Anam-ro, Seongbuk-gu, Seoul 02841, Republic of Korea*
[2]*Department of Construction and Disaster Prevention Engineering, Daejeon University Daejeon 34520, Republic of Korea*

(Received March 24, 2022, Revised July 3, 2022, Accepted July 5, 2022)

Abstract. This study characterizes Proctor and geophysical properties in a broad range of grading and fines contents. The results show that soil index properties such as uniformity and fines plasticity control the optimum water content and peak dry unit trends, as well as elastic wave velocity. The capillary pressure at a degree of saturation less than S = 20% plays a critical role in determining the shear wave velocity for poorly graded sandy soils. The reduction in electrical resistivity with a higher water content becomes pronounced as the water phase is connected A parallel set of compaction and geophysical properties of sand-kaolinite mixtures reveal that the threshold boundaries computed from soil index properties adequately capture the transitions from sand-controlled to kaolinite-controlled behavior. In the transitional fines fraction zone between $F_F \approx 20$ and 40%, either sand or kaolinite or both sand and kaolinite could dominate the geophysical properties and all other properties associated with soil compaction behavior. Overall, the compaction and geophysical data gathered in this study can be used to gain a first-order approximation of the degree of compaction in the field and produce degree of compaction maps as a function of water content and fines fraction.

Keywords: compaction; geophysical methods; threshold fines fraction; transitional behavior

1. Introduction

Compaction quality control is critical in many engineering projects (Kim *et al.* 2011, Kim *et al.* 2013) including highways, railroads, airports, and construction sites subjected to high loads (Altay *et al.* 2021, Song *et al.* 2022). Compaction is a fundamental and underlying stage for successful engineering projects. Well-controlled field compaction tends to minimize ground settlement and avoid collapse of the surface layer. In general, there are two typical compaction assessment methods: the field density measurement test (e.g., using the sand replacement method or a soil density gauge) and the plate load test.

However, high uncertainties often arise when conducting a compaction quality assessment in the field (Gong *et al.* 2021, Liu *et al.* 2021). For example, the degree of compaction for a soil composed of coarse particles tends to be overestimated when the in-situ soil density is directly compared to the density obtained from a Proctor test as the density of coarse grains is higher in comparison to the soil density (Yoo *et al.* 2018). An accurate evaluation of compaction quality remains challenging. Therefore, continuous efforts have been made toward investigating the compaction characteristics and the degree of compaction using non-destructive methods (Kim *et al.* 2011, Kim *et al.* 2013).

Underlying mechanisms for non-destructive methods often involve the multiphysics low-perturbation that facilitates comprehensive granular material characterization and process monitoring (Santamarina *et al.* 2020, Fu and Tang 2021). In particular, the characteristics of elastic waves appear to be a good indicator when determining the degree of compaction in compacted clays, particularly in compacted clay liners where an accurate prediction of the degree of compaction is critical and a geophysical assessment could be cost-effective (Daniel and Benson 1990, Daniel and Wu 1993, Patel *et al.* 2020). Non-destructive geophysical methods are simple but robust tools to assess the degree of compaction across different sediment types.

This study aims to characterize the Proctor compaction curve and geophysical properties for compacted soils with a broad range of grading and fine contents. In particular, it aims to extend laboratory results gathered herein and data interpretation to field compaction assessments. In addition to their geophysical properties such as P- and S- wave velocities and electrical resistivity, we measure the dry unit weight of specimens with different gravimetric water

∗Corresponding author, Professor
E-mail: hyungkoo@dju.ac.kr
[a]Research Professor
[b]Professor
[c]Master's Student
[d]Ph.D. Candidate

ISSN: 2005-307X (Print), 2092-6219 (Online)

contents. Then, we analyze the data in the context of percolation thresholds for liquid and air. Next, we obtain the compaction curve and geophysical properties of sand-kaolinite mixtures as functions of fines fraction; thereafter, we show that data analyzed within a physics-inspired and data-driven volumetric and gravimetric packing framework adequately capture the distinct transition from a sand-controlled to clay-controlled trend across soil state parameters and geophysical properties. Experimental results and the interpretation of geophysical data gathered in this study can help obtain a first-order approximation of the degree of compaction in the field and produce degree of compaction maps considering gravimetric water content and fines fraction. The theoretical framework is presented first.

2. Theoretical framework

2.1 Role of fines in soil properties

2.1.1 Observations

The engineering response of a soil is controlled by both its major and minor components because soils are originally mixtures of granular materials (Carraro *et al.* 2009, Georgiannou *et al.* 1990, Salgado *et al*. 2000, Lade and Yamamuro 1997). Previous studies focusing on the roles of fines as minor components in soil mixtures reveal that the arrangement of soil particles and pore spaces dramatically changes at a specific fines fraction, which is known as the critical fines content (Choo 2013, Thevanayagam 1998, Thevanayagam 2007, Yang *et al*. 2006). However, according to the Unified Soil Classification System (USCS), mixtures classified as coarse-grained soils show a significant change in hydraulic conductivity (Indrawan *et al.* 2006, Sivapullaiah *et al*. 2000), compressibility (Monkul and Ozden 2007, Tiwari and Ajmera 2011, Simpson and Evans 2015, Watabe *et al.* 2011), small strain stiffness (Choo 2013, Lee *et al*. 2007a), and friction angle (Belkhatir *et al.* 2013, Kurata and Fujishita 1961, Kenney 1977, Tiwari and Marui 2005) even when the fines fraction is lower than 50%. These observations remind geotechnical engineers that the 50% boundary used in the USCS for the classification of coarse-grained or fine-grained soils and gravel or sand cannot reflect the role of fines in the engineering properties of soil mixtures.

2.1.2 Threshold fines fraction

A binary mixture composed of coarse and fine grains is considered when defining the threshold of the fines fraction. It is assumed that the characteristic grain size of the fine component is much smaller in comparison to the coarse component; both fine and coarse components can be extremely densely or loosely packed. We define the mass fraction of fines based on a volumetric and gravimetric analysis, where the voids of the coarse grains are completely filled with fines. Thereafter, the threshold fines fraction F_{th} can be described as follows (see mathematical details in Park and Santamarina 2017)

$$F_{th} = \frac{M_F}{M_{Total}} = \frac{M_F}{M_F + M_C} = \frac{e_C}{1 + e_C + e_F} \quad (1)$$

where M_C and M_F represent the mass of coarse and fine components, respectively, and their void ratios are e_C and e_F. The specific gravities of the coarse and fine components are $G_{S,C}$ and $G_{S,F}$, respectively. The threshold fines fraction F_{th} captures a transitional soil behavior indicating whether a given soil is a coarse- or fine-dominant mixture (Choo 2013, Thevanayagam *et al*. 2002, Yang *et al.* 2006).

2.1.3 Low and high threshold fines fractions

Two threshold fines fractions can be determined by the packing condition of the fine and coarse components. When coarse grains are densely packed and fine grains are loosely packed, a low threshold fines fraction $F_{th}|^{LOW}$ is defined as follows

$$F_{th}\Big|^{Low} = \frac{{e_C}^{\min}}{1 + {e_C}^{\min} + {e_F}^{\max}} \quad (2)$$

A high threshold fines fraction $F_{th}|^{HIGH}$ is defined when coarse grains are loosely packed and fine grains are densely packed:

$$F_{th}\Big|^{High} = \frac{{e_C}^{\max}}{1 + {e_C}^{\max} + {e_F}^{\min}} \quad (3)$$

When establishing the concept of low and high threshold fines fractions, previous studies recognized that the packing condition of smaller particles between the pores formed by the larger particles could be different from packing conditions in bulk (Park and Santamarina 2017, Park *et al*. 2018). Therefore, a correction factor α is introduced to define the data-adjusted high threshold fines fraction $F_{th}|^{H*}$ where α is 1.3 for coarse-fine mixtures (Park and Santamarina 2017)

$$F_{th}\Big|^{H*} = \frac{\alpha \cdot {e_C}^{\max}}{1 + \alpha \cdot {e_C}^{\max} + {e_F}^{\min}} \quad (4)$$

Fig. 1 shows the changes in the packing density of fine and coarse grain mixtures. To describe the microstructure of mixtures, concepts of intergranular-, equivalent intergranular-, interfine-, and equivalent interfine-void ratios with equation parameters (representing the cushioning effect) have been proposed (Mitchell 1976, Zlatovic and Ishihara 1995, Thevanayangam *et al.* 2002, Ni *et al.* 2004, Rahman *et al.* 2008). As shown in Fig. 1, the low and high threshold fines fractions divide the microstructure of mixtures into three categories: (i) at a fines fraction $F_F < F_{th}|^{LOW}$, the physical properties are dominated by the coarse grains, (ii) at a fines fraction $F_{th}|^{LOW} < F_F < F_{th}|^{H*}$ (transitional mixtures), the stiffness and strength of the mixtures may show an increase or decrease and then reach the stiffness and strength of fine grains once the fines fraction exceeds $F_{th}|^{H*}$, and (iii) at a fines fraction $F_F > F_{th}|^{H*}$, all mechanical properties are controlled by the fine grains.

Table 1 Index properties of tested soils

Property	D_{10} [mm]	D_{30} [mm]	D_{60} [mm]	C_u	C_c	% Passing #200	PL	LL	PI	USCS
Soil A	0.15	0.40	0.61	4.07	1.75	3.4	-	-	-	SP
Soil B	0.32	0.51	0.61	1.91	1.33	1.1	-	-	-	SP
Soil C	0.060	0.12	0.28	4.67	0.86	14.6	17	38	21	SC
Soil D	0.085	0.13	0.30	3.53	0.66	6.7	31	76	45	SP-SC

Note: C_u = coefficient of uniformity, C_c = coefficient of curvature

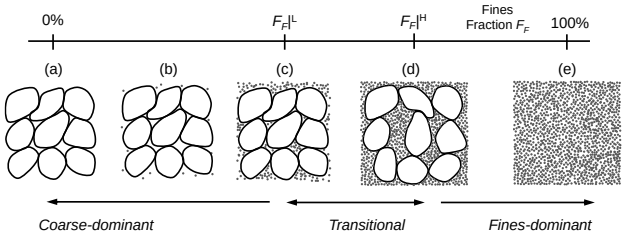

Fig. 1 Threshold fines fraction in a coarse-fine mixture with three categories: (a) Coarse grains only, (b) Mainly coarse grains, (c) Low threshold fines fraction, (d) High threshold fines fraction and (e) Fine grains only

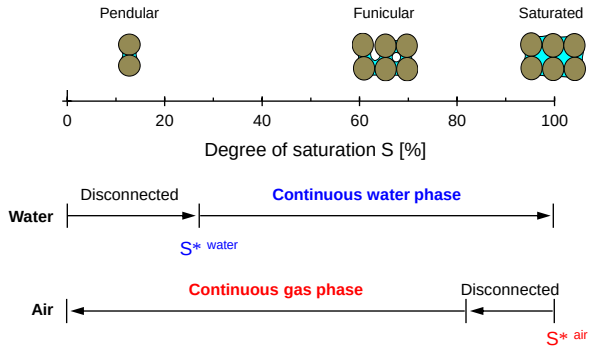

Fig. 2 Percolation threshold. The degree of saturation determines air and water connectivity through pore spaces in granular materials (Modified from Santamarina *et al*. 2001)

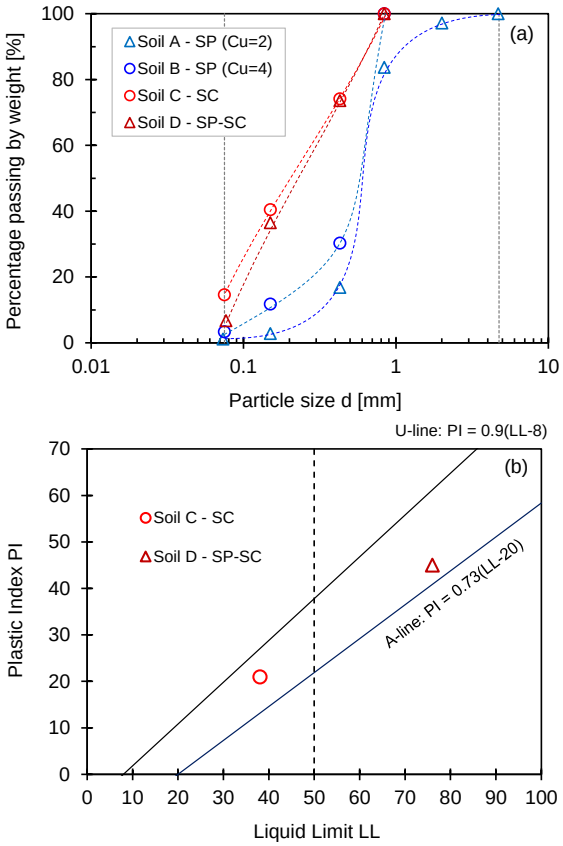

Fig. 3 Tested materials. (a) Grain size distribution curve and (b) Casagrande chart

2.2 Percolation threshold

The percolation threshold S* is the critical volume fraction of the phases when the discontinuous phase becomes connected (Fig. 2). There are two percolation thresholds: (1) water S* water ~ 25% and air S* air ~ 80%. The two thresholds vary with soil packing conditions.

3. Experimental study

3.1 Tested materials

In this study, four soil specimens are prepared for Proctor compaction tests. Fig. 3(a) plots the particle size distribution curves for all tested materials. There are two SP soils, one SC soil, and one SP-SC soil based on the USCS. The coefficient of uniformity C_u indicates that Soil A seems to be more well-graded in comparison to Soil B. Fig. 3(b) indicates that the results of plastic index, PI, and liquid limit, LL, classify Soil C as SC and Soil D as SP-SC. Table 1 summarizes all properties used for soil classification for the four tested soils.

3.2 Experimental device and configuration

This study uses a modified compaction mold to conduct B-type Proctor compaction tests of the four soils (KS F 2312, 2001). Fig. 4(a) shows the compaction mold used for geophysical soil property measurements. The height of the mold is 24 cm, and its inner diameter is 15 cm. This mold includes bender elements for S-wave (S), a piezo disk element for P-wave (P), and a needle probe for electrical resistivity (Q) measurements. There are five holes along the depth for installing geophysical measurement sensors. All sensors used for geophysical property measurements are installed on the modified compaction mold before Proctor

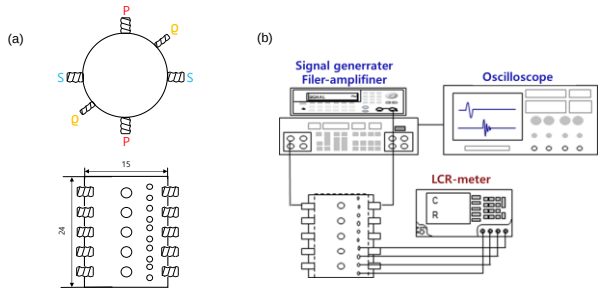

Fig. 4 Experimental device and configuration. (a) Modified compaction cell and (b) Peripheral electronics to measure P- and S-waves and electrical resistivity

compaction tests. After a complete set of Proctor compaction tests, S- and P-waves and electrical resistivity values are monitored and acquired for a compacted soil sample.

Fig. 4(b) shows the data acquisition system. For elastic wave measurements, the function generator forms step input signals with 10 V input voltage (Keysight 33210A), and elastic waves transformed by the bender element propagate through the soils. The filter-amplifier (Krohn-Hite 3364) uses frequencies of 500 Hz and 200 kHz for high- and low-pass filtering, respectively. The computer saves the signals shown on the oscilloscope (Keysight DSOX 2014A). The minimum sampling frequency of the received signals is 1 MHz. The number of signals stacked for a high signal-to-noise ratio is 1024 (Santamarina and Fratta 2005). For electrical resistivity assessments, this study uses an LCR-meter with four electrodes and a Wenner array. The LCR meter captures electrical resistance R of the soil samples where the input voltage is 1 V, and the operating frequency is 100 kHz (Agilent 4236B). The electrical resistance R measured for compacted soils is converted to electrical resistivity using a calibration factor (see detailed calibration procedure in Kim *et al*. 2011).

Proctor compaction tests start with the soils under dry conditions. Then, we conduct Proctor compaction tests of the four soils at every 3% increase in water content ω. The ionic concentration for pore water is 0.5 M for stable electrical resistance measurements.

3.3 Experimental results

3.3.1 Dry unit weight

Fig. 5 shows the dry unit weight γ_d versus water content ω for the four soils tested in this study. The dry unit weight is in the range γ_d = 12.5–16.8 kN/m^3. The optimum water content ω* represents the gravimetric water content where a soil attains the maximum dry unit weight. The optimum water content increases as the soil type changes from poorly graded sandy to more plastic clayey soils. The optimum water content appears to increase with a higher coefficient of uniformity and more plastic fines. Compaction aims to remove the air in the pores in granular materials. In this context, the peak dry unit weight is likely to be attained at a water content less than the percolation threshold for air phase in all cases.

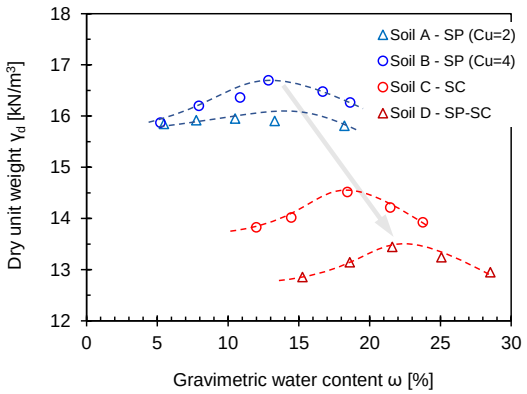

Fig. 5 Dry unit weight versus gravimetric water content for the four soils tested in this study

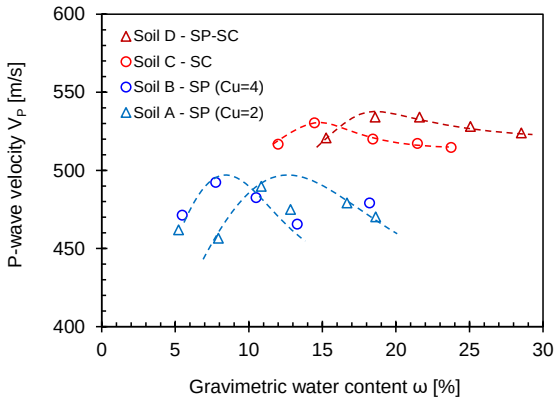

Fig. 6 P-wave velocity versus gravimetric water content for the four soils tested in this study

3.3.2 P-wave velocity

Fig. 6 plots P-wave velocity V_p versus water content ω for the four tested soils. The P-wave velocity for the tested soils is in the range V_p = 450–540 m/s, which is below the typical P-wave velocity for water, i.e., V_p = 1450 m/s. This observation indicates that all compacted soils are under unsaturated conditions. The P-wave velocity for clayey sands tend to be higher in comparison to the poorly graded sands. The water content corresponding to the peak P-wave velocity is likely to increase with a smaller coefficient of uniformity and more plastic fines in the soil mixture.

3.3.3 S-wave velocity

Fig. 7 plots shear wave velocity V_s against water content ω for the four tested soils. In general, the S-wave velocity tends to decrease with water content. A gravimetric-volumetric relationship $S{\cdot}e = \omega{\cdot}G_s$ can be used to convert the gravimetric water content ω to the degree of saturation S, where e is the void ratio and G_s is the specific gravity. This packing analysis reveals that the capillary pressure built up at a degree of saturation less than S = 20% plays a critical role in determining the shear wave velocity for the poorly graded sandy soils A and B. In particular, the coefficient of uniformity C_u controls the packing density and pore size distribution. Then, a higher C_u leads to denser packing and smaller pore size. Therefore, the shear wave velocity for soil B is greater in comparison to soil A, across

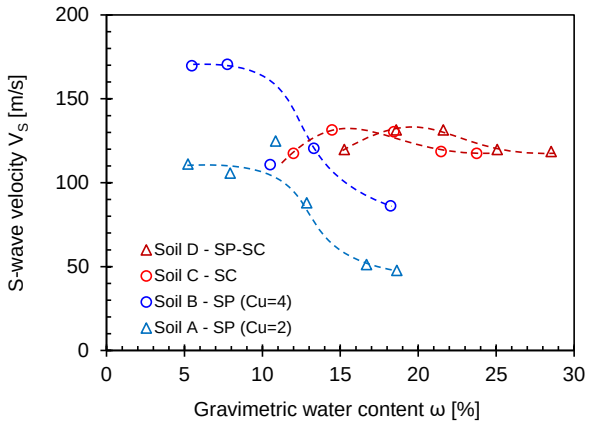

Fig. 7 S-wave velocity versus gravimetric water content for the four soils tested in this study

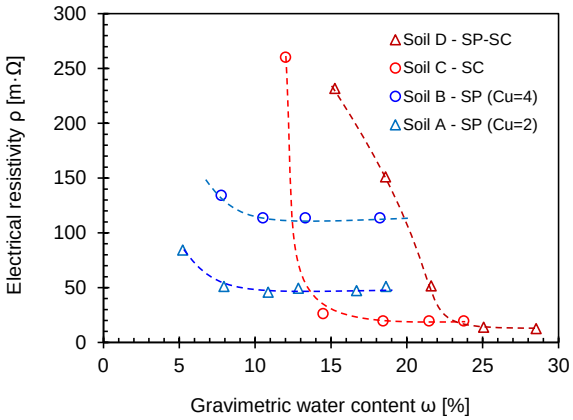

Fig. 8 Electrical resistivity versus gravimetric water content for the four soils tested in this study

the entire water content range under consideration. The capillary pressure diminishes and the shear wave velocity decreases as the soils A and B move closer to a fully saturated state (see similar observations in Kim *et al.* 2021). By contrast, the shear wave velocities for the clayey sandy soils C and D are not sensitive to the water content, and they are relatively higher in comparison to soils A and B. This trend may be a result of the cohesion of fines in soils C and D.

3.3.4 Electrical resistivity

Fig. 8 plots the electrical resistivity of the four soils as a function of water content. The electrical resistivity remains high at a relatively low water content in all cases. However, the reduction in electrical resistivity with a higher water content becomes pronounced as the water phase becomes connected. The electrical resistivity data indicate that when the ionic concentration of the pore fluid is high, pore water conduction rather than particle conduction appears to be critical for electrical conduction phenomena in the granular materials. Then, pore size plays a crucial role in the determination of electrical resistivity. The poorly graded sandy soils A and B tend to have relatively uniform and larger pores in comparison to the clayey soils C and D. Therefore, at a low water content, the electrical resistivities of soils A and B are lower compared to those of C and D.

4. Analyses and discussion

4.1 Comparison

Fig. 9 shows the variation in the water content ω* of the four test soils that matches with the peak value for each measurement including proctor compaction, S-wave velocity, P-wave velocity, and electrical resistivity. In general, the peak electrical resistivity value appears at the lowest water content where air phase is connected. The addition of a small amount of water leads to unsaturated conditions and there exists capillary pressure that enhances the particle contact force. These particle scale phenomena result in the peak value for the P- and S-wave velocity at a middle range of water content ω*. Finally, the comparison in Fig. 9 highlights that the proctor compaction requires the most significant water content to achieve peak dry density. The volumetric and gravimetric analysis indicates that the optimum water content for proctor compaction is near the percolation threshold for the liquid phase. Geophysical data accumulated for the various soil types and water contents will help us anticipate the degree of compaction where the value of the water content, at which peak dry density occurs, is greater in comparison with the water content for peak values of geophysical properties.

4.2 Sand-kaolinite mixtures - Role of fines in geophysical properties

In this study sand-kaolinite mixtures with fines fractions of 0, 10, 20, 40, 60, and 100% by weight were prepared. Then, we gathered the compaction curve and geophysical properties of sand-kaolinite mixtures. Fig. 10 shows the typical compaction curve for the sand-kaolinite mixtures with the six different fines fractions. The peak unit density γ_d increases and the optimum water content decreases as the fines fraction increases from F_F = 0 to 20%. Thereafter, the peak unit density γ_d decreases and the optimum water content significantly increases with higher fines fractions. Clearly, there is a transitional behavior in the proctor compaction test that varies with kaolinite content.

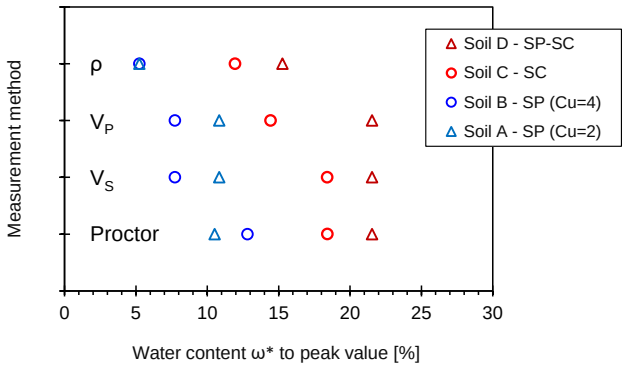

Fig. 9 Variation of water content corresponding to peak value for each measurement such as proctor compaction, S-wave velocity V_s, P-wave velocity V_p, and electrical resistivity ρ

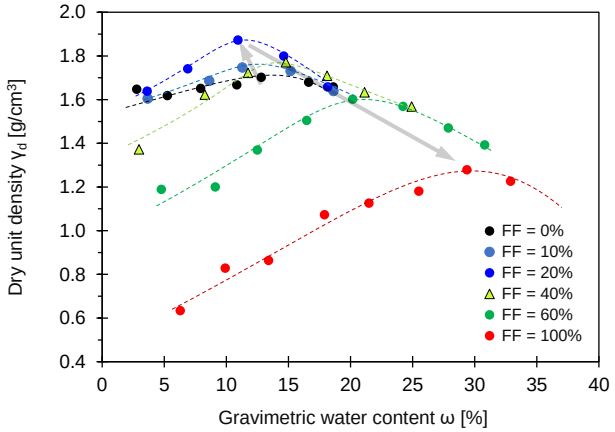

Fig. 10 Typical compaction curve for sand-kaolinite mixtures. F_F indicates the fines fraction by weight

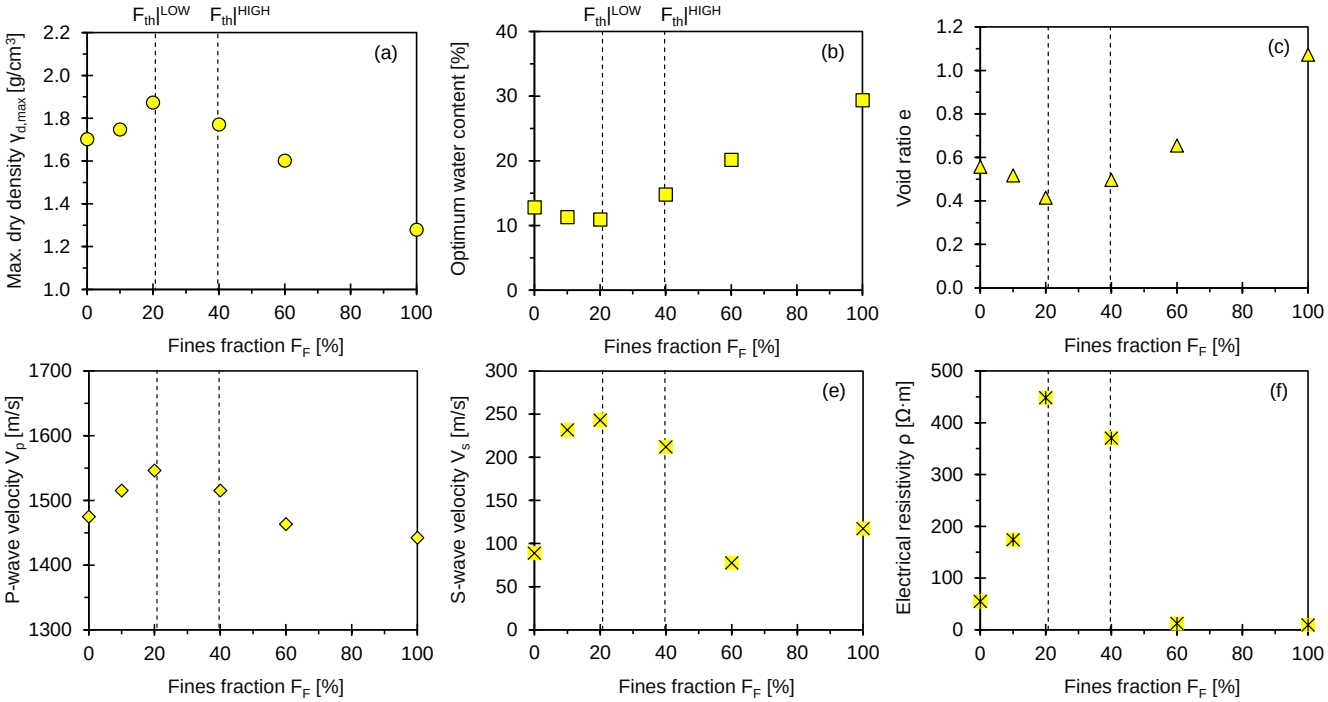

Fig. 11 Soil state parameters and geophysical properties as functions of fines fraction. (a) Maximum dry density, (b) Optimum water content, (c) Void ratio, (d) P-wave velocity, (e) S-wave velocity, and (f) Electrical resistivity. The input parameters used for the computation of low $F_{th}|^{LOW}$ and data-adjusted high threshold $F_{th}|^{H*}$ fines fractions include e_C^{min} = 0.647, e_C^{max} = 0.913, and liquid limit of kaolinite LL = 54, where $F_{th}|^{LOW}$ = 20.7% and $F_{th}|^{H*}$ = 39.6%. The maximum and minimum void ratio of kaolinite are estimated based on the liquid limit *LL* where $e_F^{max} = e_F|^{10kPa} = 0.026 \cdot LL + 0.07$ and $e_F^{min} = e_F|^{1MPa} = 0.011 \cdot LL + 0.21$ (see details in Park and Santamarina 2017)

Fig. 11 shows the maximum dry density $\gamma_{d,max}$, optimum moisture content OMC, void ratio, P-wave velocity, S-wave velocity, and electrical resistivity obtained at maximum dry density $\gamma_{d,max}$ and optimum moisture content OMC as a function of the fines fraction F_F (see Fig. 10). The transition boundaries computed from soil index properties such as e_{max}, e_{min}, and LL are superimposed in each property where $F_{th}|^{LOW}$ = 20.7% and $F_{th}|^{H*}$ = 39.6% ((Eqs. (2)-(4) – see detailed computation procedure in Park and Santamarina 2017). From the figure it is evident that, the threshold fines fractions properly capture the transitions from sand-controlled to kaolinite-controlled data trend. In the transitional zone between $F_F \approx 20$ and 40%, either sand, kaolinite or both components could be in charge of the geophysical properties and all properties associated with compaction tests. A previous study also shows the similar P-and S-wave velocity data as a function of kaolinite fraction in sand-kaolinite mixtures (Vallejo and Lobo-Guerrero 2005). This trend supports the reliability of geophysical data obtained in this study. Data analyzed within a physics-inspired and data-driven volumetric and gravimetric packing framework indicate that the

interpretation of geophysical and compaction data conducted in this study can be used to gain a first-order approximation of the degree of compaction in the field and to produce degree of compaction maps considering water content and fines fraction.

Figs. 10 and 11 clearly show the transition behavior at fines fraction F_F = 20-to-40%. These observations indicate that the transitional behavior for a soil mixture is soil-specific based on their index properties. Therefore, the accurate prediction of the low and high threshold fines fraction and well-controlled laboratory compaction tests will help geotechnical engineers anticipate the geophysical properties of compacted soils together with degree of compaction in the field.

5. Conclusions

Compaction quality control plays a critical role in many engineering projects. This study aimed to characterize the Proctor compaction curve and investigate the variation in the geophysical properties of compacted soils with a broad range of grading and fines contents. From the perspective of granular packing, we also investigated a parallel set of compaction characteristics and geophysical properties of sand-kaolinite mixtures as a function of their fines fraction. The following conclusions were drawn.

The optimum water content is likely to increase with a higher coefficient of uniformity and higher fines plasticity. The peak dry unit weight obtained from the compaction test appears at a water content less than the percolation threshold for the air phase in all cases. The P-wave velocity of clayey sands tends to be higher compared to that of the poorly graded sands. The water content corresponding to the peak P-wave velocity appears to increase with a smaller coefficient of uniformity and more plastic fines in the soil mixture.

The capillary pressure at a degree of saturation less than S = 20% plays a critical role in the determination of shear wave velocity for poorly graded sandy soils. In particular, the coefficient of uniformity C_u controls the packing density and pore size distribution. Then, a higher C_u leads to denser packing and smaller pore size.

The electrical resistivity remains high at a relatively low water content in all cases. However, the reduction in electrical resistivity with a higher water content becomes pronounced as the water phase becomes connected.

The transition boundaries computed from soil index properties, such as maximum and minimum void ratios and liquid limit, can adequately capture the transitions from the sand-controlled to the kaolinite-controlled data trend. In the transitional zone between $F_F \approx 20$ and 40%, either sand, kaolinite, or both sand and kaolinite can dominate the geophysical properties and all other properties associated with soil compaction.

Data analyzed within a physics-inspired and data-driven volumetric and gravimetric packing framework can adequately capture the distinct transition from the sand-controlled to the clay-controlled trends across soil state parameters and geophysical properties. Experimental results and the interpretation of geophysical data gathered in this study can help obtain a first-order approximation of the degree of compaction in the field and produce degree of compaction maps considering water content and fines fraction.

Acknowledgments

This work was supported by the National Research Foundation of Korea (NRF) grant funded by the Korea government (MSIT) (No. NRF-2021R1A5A1032433) and Basic Science Research Program through the National Research Foundation of Korea (NRF) funded by the Ministry of Education (No. NRF-2020R1A2C2012113).

References

Altay, G., Kayadelen, C., Canakci, H., Bagriacik, B., Ok, B. and Oguzhanoglu, M.A. (2021), "Experimental investigation of deformation behavior of geocell retaining walls", *Geomech. Eng.*, **27**(5), 419-431. https://doi.org/10.12989/gae.2021.27.5.419.

Castro, G.M., Park, J. and Santamarina, J.C (2022), "Revised soil classification system RSCS: Implementation and engineering implications", *J. Geotech. Geoenviron. Eng*., (Under review).

Daniel, D.E. and Benson, C.H. (1990), "Water content-density criteria for compacted soil liners", *J. Geotech. Eng.*, **116**(12), 1811-1830. https://doi.org/10.1061/(ASCE)0733-9410(1990)116:12(1811).

Daniel, D.E. and Wu, Y.K. (1993). "Compacted clay liners and covers for arid sites", *J. Geotech. Eng.*, **119**(2), 223-237. https://doi.org/10.1061/(ASCE)0733-9410(1993)119:2(223).

Fu, B. and Tang, C.A. (2021), "Acoustic emission characteristics of marble under uniaxial cyclic loading", *Geomech. Eng.*, **27**(4), 347-359. https://doi.org/10.12989/gae.2021.27.4.347.

Gong, J., Cheng, L., Zhao, L., Zou, J., Li, L. and Nie, Z. (2021), "Study on the packing and shear characteristics of granular mixtures via the DEM", *Geomech. Eng.*, **27**(3), 223-237. https://doi.org/10.12989/gae.2021.27.3.223.

Kim, H.S., Jung, Y.H., Gang, D.Y. and Lee, S.H. (2011), "Evaluation of degree of compaction of railroad trackbed fills using elastic wave velocities", *Proceedings of the Korean Society for Railway Conference*.

Kim, J.H., Yoon, H.K. and Lee, J.S. (2011), "Void ratio estimation of soft soils using electrical resistivity cone probe", *J. Geotech. Geoenviron. Eng.*, **137**(1),86-93.

Kim, J., Won, J. and Park, J. (2021), "Effects of water saturation and distribution on small-strain stiffness", *J. Appl. Geophys.*, **186**, 104278. https://doi.org/10.1016/j.jappgeo.2021.104278.

Kim, K.S., Woo, W., Lee, C. and Lee, W. (2013), "Laboratory soil box tests for compaction characteristics of foundation soils using nondestructive and penetration tests", *J. Korean Soc. Hazard Mitigation*, **13**(5), 93-101. https://doi.org/10.9798/KOSHAM.2013.13.5.093.

KS F 2312 (2001), Test method for soil compaction using a rammer, Korean Standards Association, Seoul, South Korea. (in Korean).

Liu, S., Wang, Y. and Feng, D. (2021), "Numerical research on two-dimensional bridge formation at the cohesionless sand-geotextile interface with the DEM method". *Geomech. Eng.*, **27**(3), 263-271. https://doi.org/10.12989/gae.2021.27.3.263.

Park, J. and Santamarina, J.C. (2017), "Revised soil classification system for coarse-fine mixtures", *J. Geotech. Geoenviron. Eng.*,

143(8), 04017039. https://doi.org/10.1061/(asce)gt.1943-5606.0001705.

Park, J., Castro, G.M. and Santamarina, J.C. (2018), "Closure to "Revised soil classification system for coarse-fine mixtures", *J. Geotech. Geoenviron. Eng.*, **144**(8), 07018019. https://doi.org/10.1061/(asce)gt.1943-5606.0001705.

Patel, A., Ingale, R. and Mandal, A. (2020), "Measurement of wave velocities in compacted clay using bender/extender and accelerometer: An experimental and numerical approach", *Measurement*, **157**, 107676. https://doi.org/10.1016/j.measurement.2020.107676.

Santamarina, J.C., Garcia, A., Hakiki, F., Park, J. and Zhao, B. (2020), "Multiphysics low-perturbation methods for sediment characterization and process monitoring", *Proceedings of the 5th International Conference on Engineering Geophysics (ICEG)*, Society of Exploration Geophysicists.

Song, S.H., Cho, D.S. and Seo, S.G. (2022), "Reinforcement effect of surface stabilizer using surface curtain walls on aging reservoirs", *Geomech. Eng*., **28**(1), 1-10. https://doi.org/10.12989/gae.2021.28.1.001.

Vallejo, L.E. and Lobo-Guerrero, S. (2005), "The elastic moduli of clays with dispersed oversized particles", *Eng. Geol*., **78**(1-2), 163-171. https://doi.org/10.1016/j.enggeo.2004.12.003.

IC